



## Study of Molecular Docking, Physicochemical and Pharmacokinetic Properties of GSK-3 $\beta$ Inhibitors

Leide C. S. Picanço<sup>1</sup>, Leandro L. Castro<sup>1</sup>, Abraão A. Pinheiro<sup>1</sup>,  
Karina R. da Silva<sup>1</sup>, Lucilene R. de Souza<sup>1</sup>, Francinaldo S. Braga<sup>1</sup>,  
Carlos H. T. P. da Silva<sup>2</sup>, Cleydson B. R. Santos<sup>1,2</sup> and Lorane I. S. Hage-Melim<sup>1\*</sup>

<sup>1</sup>Laboratory of Modeling and Computational Chemistry, Federal University of Amapá, Macapá, Amapá 68902-280, Brazil.

<sup>2</sup>Computational Laboratory of Pharmaceutical Chemistry, School of Pharmaceutical Sciences of Ribeirão Preto, University of São Paulo, Ribeirão Preto, São Paulo, 14040-903, Brazil.

### Authors' contributions

*This investigation was performed in collaboration with all authors. Authors LCSP, LLC and LISHM designed the study, wrote the protocol, involved in writing the first draft, participated in data collection.*

*Authors AAP, KRS, LRS and FSB managed the literature search, analyses of the study and manuscript preparation. Authors CHTPS, CBRS and LISHM performed data interpretation and were actively involved in reading the manuscript. All authors read and approved the final manuscript.*

### Article Information

DOI: 10.9734/BJPR/2015/18054

#### Editor(s):

(1) Mohamed Fathy, Assiut University, Assiut, Egypt.

#### Reviewers:

(1) Hazem Mohammed Ebraheem Shaheen, Department of Pharmacology, Damanhour University, Egypt.

(2) Arturo Solis Herrera, Human Photosynthesis Research Center, Mexico.

Complete Peer review History: <http://www.sciencedomain.org/review-history.php?id=1178&id=14&aid=9586>

**Original Research Article**

**Received 1<sup>st</sup> April 2015**  
**Accepted 5<sup>th</sup> May 2015**  
**Published 4<sup>th</sup> June 2015**

### ABSTRACT

**Aims:** Alzheimer disease (AD) affects people aged 65 to 90 years and is the most prevalent neurodegenerative disease in the world. The deposition of  $\beta$ -amyloid peptide forming the amyloid plaques as well as neurofibrillary tangles deposition due to hyperphosphorylation of tau protein are the major cause of the disease in addition to the deficit of the neurotransmitter acetylcholine in the synaptic gap. Among the treatments for AD are acetylcholinesterase, beta-secretase and Glycogen Synthase Kinase-3 $\beta$  (GSK-3 $\beta$ ) inhibitors. GSK-3 $\beta$  has been associated with all primary abnormalities of AD, because it interacts with the different components of the amyloid plaques production system and participates in the phosphorylation of tau protein. This regulates and stabilizes the microtubules in axons of the neurons of the Central Nervous System (CNS). The

\*Corresponding author: Email: [lorane@unifap.br](mailto:lorane@unifap.br);

present study aimed to propose three novel candidates for inhibitors of GSK-3 $\beta$ .

**Place and Duration of Study:** Laboratory of Modeling and Computational Chemistry (LMCC) at Federal University of Amapá (UNIFAP), Macapá, Brazil, between November 2014 and March 2015.

**Methodology:** First, we used the crystal structure of GSK-3 $\beta$  enzyme deposited in the the Protein Data Bank (PDB) (PDB ID: 3Q3B – at 2.7 Å resolution). Then, we selected 50 inhibitors reported and available in the database BindingDB. Docking simulations were subsequently carried out using the AutoDock Vina 1.5.6 software. In sequence, a pharmacophore perception calculation was performed as well as and pharmacokinetic properties calculations. Finally, new proposals of GSK-3 $\beta$  inhibitors candidates were designed, considering in addition potential biological activity and synthetic accessibility as well as.

**Results:** In the study of physical and chemical parameters, most of the compounds violated no more than two parameters of the Lipinski's Rule of five, indicating suitable oral absorption. Along of the docking simulations, 22 inhibitors showed strong interaction with the amino acid residues of the enzyme active site (hydrogen bond and hydrophobic interactions). Along of the pharmacophore perception calculation, 30 molecules lined up with four pharmacophore points: two aromatic rings and two hydrogen bond acceptor groups (in the case, pyrimidine group). Along the prediction of pharmacokinetics, the most of the potential GSK-3 $\beta$  inhibitors showed good permeability of Caco2 and MDCK cells, high absorption in the human intestine and weak binding to plasma proteins, but only two ones showed absorption in the blood brain barrier. The three proposals of GSK-3 $\beta$  inhibitor candidates indicate biological activity for GSK-3 $\beta$ , as well as having average synthetic accessibility.

**Conclusion:** This current study reveals three new promising compounds with *in silico* GSK-3 $\beta$  inhibitory activity. Therefore, further studies of quantitative structure-activity relationship as are necessary to investigate how the chemical structures of these molecules affect their biological potency and binding affinity for GSK-3 $\beta$  enzyme, and thus, selecting potential drug candidates for synthesis and biological testing.

**Keywords:** Alzheimer's disease; GSK-3 $\beta$  inhibitors; *in silico* drug design; docking molecular; pharmacophore derivation; ADME; prediction of activity; synthetic accessibility.

## 1. INTRODUCTION

In neurodegenerative diseases occurs in general a change of protein conformation leading to aggregation, thus causing a cascade of events that result in loss of both connectivity and plasticity of neurons. Such diseases mainly affect people with advanced age but the events that trigger their origin is still unclear [1,2].

Among these diseases are Alzheimer's disease (AD), which is the most prevalent degenerative disorder and cause of dementia in the world, reaching about 1.5% of the population aged 65-69 years, 21% between 85 and 86 years and 39% over 90 years. In Brazil, about 6% of the population over 60 shows symptoms of the disease [3-6].

AD was first related by the german doctor Alois Alzheimer in 1906, when he diagnosed the patient Auguste Deter with a neurological condition not known. After the death of such patient, Dr. Alois performed the autopsy of his brain and found the current trademark of the

disease: amyloid plaques and neurofibrillary tangles [6-8].

Amyloid plaques are formed by the deposition of the  $\beta$ -amyloid peptide after abnormal proteolytic processing of the amyloid precursor protein (APP) by  $\beta$ - and  $\gamma$ -secretase enzymes [9-12]. This accumulation subsequently yields senile plaques. On the other hand, neurofibrillary tangles are formed inside the nervous cells, due to the large production of hyperphosphorylated Tau protein. Tau protein stabilizes microtubules, fundamental members of cytoskeleton of the axons, which are mainly responsible for maintaining the neuronal structure and transport of various substances such as neurotransmitters [9-12].

In addition to the above mentioned, the pathophysiology of AD is also associated with reduction in levels of acetylcholine (ACh) in synapses, resulting in the decrease of the cortical cholinergic neurotransmission, also leading to changes in other neurotransmitters such as dopamine, noradrenaline, serotonin and other ones [13].

In the early stages of AD, there is loss of episodic memory and difficulty in acquiring new tasks. This damage gradually also involves judgment, abstraction and visuospatial skills. In the terminal phase of the disease, changes of the sleep cycle and behaviour are also detected, as well as inability to walk, talk, etc [14,15].

For current AD treatment, acetylcholinesterase inhibitors (AChEi) are clinically used, whose enzyme is responsible for the hydrolysis of ACh into choline and acetate, resulting in increased levels of such neurotransmitters in the synaptic gap [13,16]. Another alternative currently explored is the use of secretase inhibitors, which should block the action of the proteolytic enzymes involved in the cleavage of the APP, thus reducing the formation of  $\beta$ -amyloid peptide [17].

Glycogen synthase kinase-3 (GSK-3) is a serine/threonine kinase with two isoforms,  $\alpha$  and  $\beta$ , involved in the regulation of various processes [18,19]. This enzyme has been associated with all primary abnormalities related to AD, where it interacts with the different components of the amyloid plaques production system and participates in the phosphorylation of tau protein [20-23].

In this present work, we aimed to propose novel GSK-3 $\beta$  inhibitors candidates for AD future treatment, using current molecular modeling and drug design approaches.

## 2. METHODOLOGY

### 2.1 Search for Therapeutic Target and Inhibitors

GSK-3 $\beta$  was selected since it plays an important role in the AD pathology. First, it was necessary to download the PDB file (<http://www.pdb.org>) of the human GSK-3 $\beta$  structure (PDB ID: 3Q3B - at 2.7Å resolution) in complex with the inhibitor 4-(4-hydroxy-3-methylphenyl)-6-phenylpyrimidin-2(5H)-one [24]. In sequence, a search for inhibitors with known and reported activity for GSK-3 $\beta$  enzyme was performed on the BindingDB database ([www.bindingdb.org/bind/index.jsp](http://www.bindingdb.org/bind/index.jsp)) [25]. 50 molecules with highest inhibitory activity (Ki) were selected. After downloading the inhibitors structures, each molecule was geometry optimized and energy was full minimized using the semiempirical Hamiltonian RM1 (Recife Model 1), thus implemented in the HyperChem v. 8.0.6 software [26].

### 2.2 Molecular Docking Procedures

Molecular docking investigates the possible orientations that a molecule assumes inside the binding site of a receptor, proposing a suitable and potential binding mode for it. A function score is used to rank the best fitted ones, and it is based on a empirical energy function containing electrostatic, van der Waals, hydrogen bonds and hydrophobic parameters [27,28].

For docking simulations, hydrogen atoms were previously added and oriented to the GSK-3 $\beta$  enzyme structure here used. The Vina 1.5.6 AutoDock software [29] was used with each GSK-3 $\beta$  inhibitor. Vina uses an automatic procedure to predict the interaction of ligands with the biomolecular target. A validation of the docking was performed by calculating the RMSD (Root Mean-Square-Deviation) between the inhibitor and the pose (conformation plus orientation) of highest score resulting: the top-ranked solution. The Grid Box was centered in Lys85, Asp133 and Val135 residues [24], with the following values  $x = 40.586$ ,  $y = 9.722$  and  $z = 38.614$ .

### 2.3 Pharmacophore Perception

A pharmacophore hypothesis was generated from the PharmaGist server (<http://bioinfo3d.cs.tau.ac.il/PharmaGist/>) using the 32 most active GSK-3 $\beta$  inhibitors there reported amongst the 50 selected from such web database [30].

Molecular interactions predictions is the primary goal of the "active analog paradigm" strategy on rational drug design. A pharmacophore describes the structural arrangement of the essential molecular characteristics of an interaction between a ligand and its receptor. A pharmacophoric interaction can be elucidated from a set of known active ligands by identifying a pharmacophore consensus that is conformationally accessible to all binders [31].

### 2.4 ADME Screening

ADME (Absorption, Distribution, Metabolism and Excretion) prediction was performed using the PreADMET server (<http://preadmet.bmdrc.org/>) [32]. Pharmacokinetic properties of the structures can predict permeability of Caco-2 cells, MDCK cells, BBB (blood brain barrier), HIA (human intestinal absorption). Yamashita et al. states that these cells have been recommended as an *in*

*vitro* model of confidence for the prediction of oral absorption of the drug candidate [33].

## 2.5 Prediction of Activity and Synthetic Accessibility for the Novel Proposals

From the data obtained *in silico* it was possible to propose changes in the structure of the reported hits and thus predict their pharmacokinetic properties, such as described above. Furthermore, it was also possible to predict the synthetic accessibility of the novel proposals and compare the results with those obtained for the reference GSK-3 $\beta$  inhibitors, using the online program SYLVIA ([http://www.molecular-networks.com/online\\_demos/sylvia/](http://www.molecular-networks.com/online_demos/sylvia/)) [34]. Activity prediction was *in silico* performed using the PASS (<http://www.akosgmbh.de/pass/index.html>) web software, which predicts with high accuracy (70-80%) up to 2000 chemical compounds for biological activities [35].

## 3. RESULTS AND DISCUSSION

The 50 most active GSK-3 $\beta$  inhibitors were selected from the BindingDB database (Fig. 1). Table 1 contains the selected inhibitors and their respective structural parameters for the theoretical analysis of oral bioavailability profiles under the Lipinski's Rule (RO5).

According to Lipinski et al. [36], for a drug to exhibit good oral bioavailability, it must meet at least three of the following parameters: molecular weight less than or equal to 500 Daltons (Da), high lipophilicity (LogP of less than 5), number of hydrogen donors smaller 5 and number of hydrogen acceptors less than 10.

Most of the selected inhibitors did not violate the Lipinski rule. Inhibitors 2 and 16 have molecular weight higher than 500, and compound 16 has 12 hydrogen bond acceptors, and 2 violations of RO5. Inhibitor 11 has more than 10 hydrogen bond acceptors, and inhibitor 50 had log P higher than 5.

Almeida et al. investigated the physicochemical properties included in RO5 for AChE inhibitor compounds, and they found that most of the compounds have no more than one violation of the rule, indicating a good oral availability according to Lipinski's Rule [28].

In order to perform docking calculations, selected GSK-3 $\beta$  structure deposited in the PDB (PDB ID: 3Q3B) was used with the AutoDock v.1.5.6

software [29]. The water molecules, the chain B and the inhibitor were withdrawn from the complex and subsequently hydrogens atoms and partial Gasteiger-Marsili charges were added. Then, the preparation of the inhibitor 4-(4-hydroxy-3-methylphenyl)-6-phenylpyrimidin-2(5h)-one was carried out. After docking simulation, the validation of the result was made by calculating the RMSD (Root-Mean-Square Deviation, of 0.8352 Å) between the experimental crystallographic pose and the top-ranked docking solution obtained for the same inhibitor (Fig. 2).

According to Cole et al. [37] prediction of the binding mode using docking, with RMSD less than 2 Å regarding the crystallographic pose of the ligand is deemed successful. The overlap of the best pose of the inhibitor N-(4-methoxybenzyl) -N'-(5-nitro-1,3-thiazol-2-yl) urea after docking with the crystallographic one of GSK-3 $\beta$  (PDB ID: 1Q5K) shows a RMSD of 0.7460 Å, second Darshit et al. [38].

The RMSD between the top-ranked docking solution and the crystallographic pose of the inhibitor acid 2-chloro-5-[4-(3-chloro-phenyl)-2,5-dioxo-2,5-dihydro-1H-pyrrol-3-ylamino] benzoic and the result of docking with GSK-3 $\beta$  (PDB ID: 1Q4L) is 1.45 Å. This ligand interacts with residues Asp133, Val135, Arg141 and Gln185 of the enzyme [39].

Docking simulations were carried out for all the 50 inhibitors, but we selected only inhibitors which showed interaction with the active site amino acids and, among them, those having a higher number of interactions. Analyses showed that conventional and non-conventional hydrogen bonds and hydrophobic interactions were observed between residues Lys85, Asp133 and Val135 of the enzyme and most inhibitors (Fig. 3).

Conventional hydrogen bonds are characterized by when a proton acceptor molecule interacts with a proton donor molecule due to the electronegativity difference. This type of coupling occurs between electronegative atoms such as fluorine, oxygen and nitrogen. On the other hand, the non-conventional hydrogen bonds occur between atoms with high electronegativity (donor or acceptor) and carbons (through  $\pi$  electrons) [40-42]. Table 2 shows the distances (in Ångströms) between amino acids of the GSK-3 $\beta$  active site and selected inhibitors.

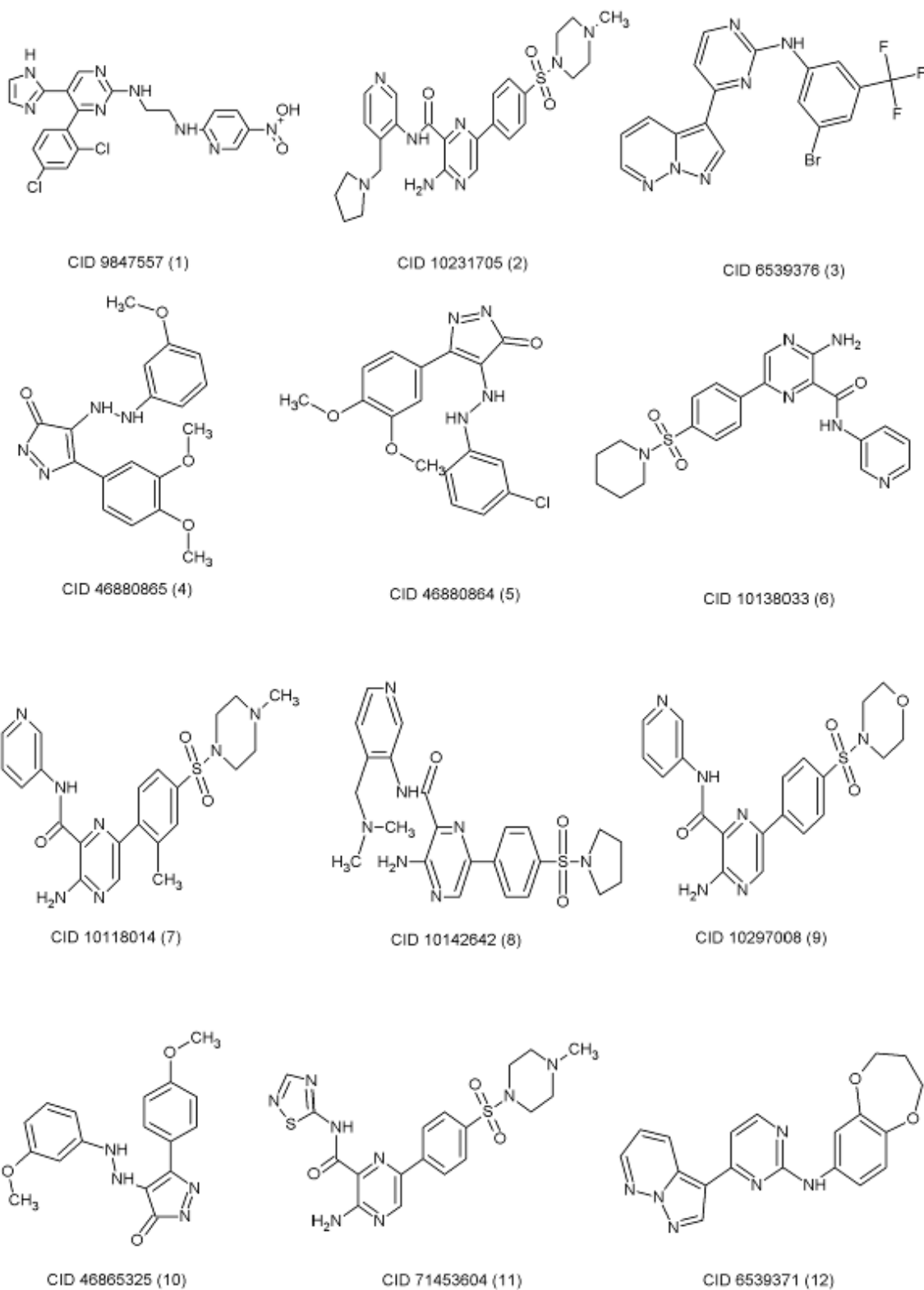


Fig. 1. Continuation

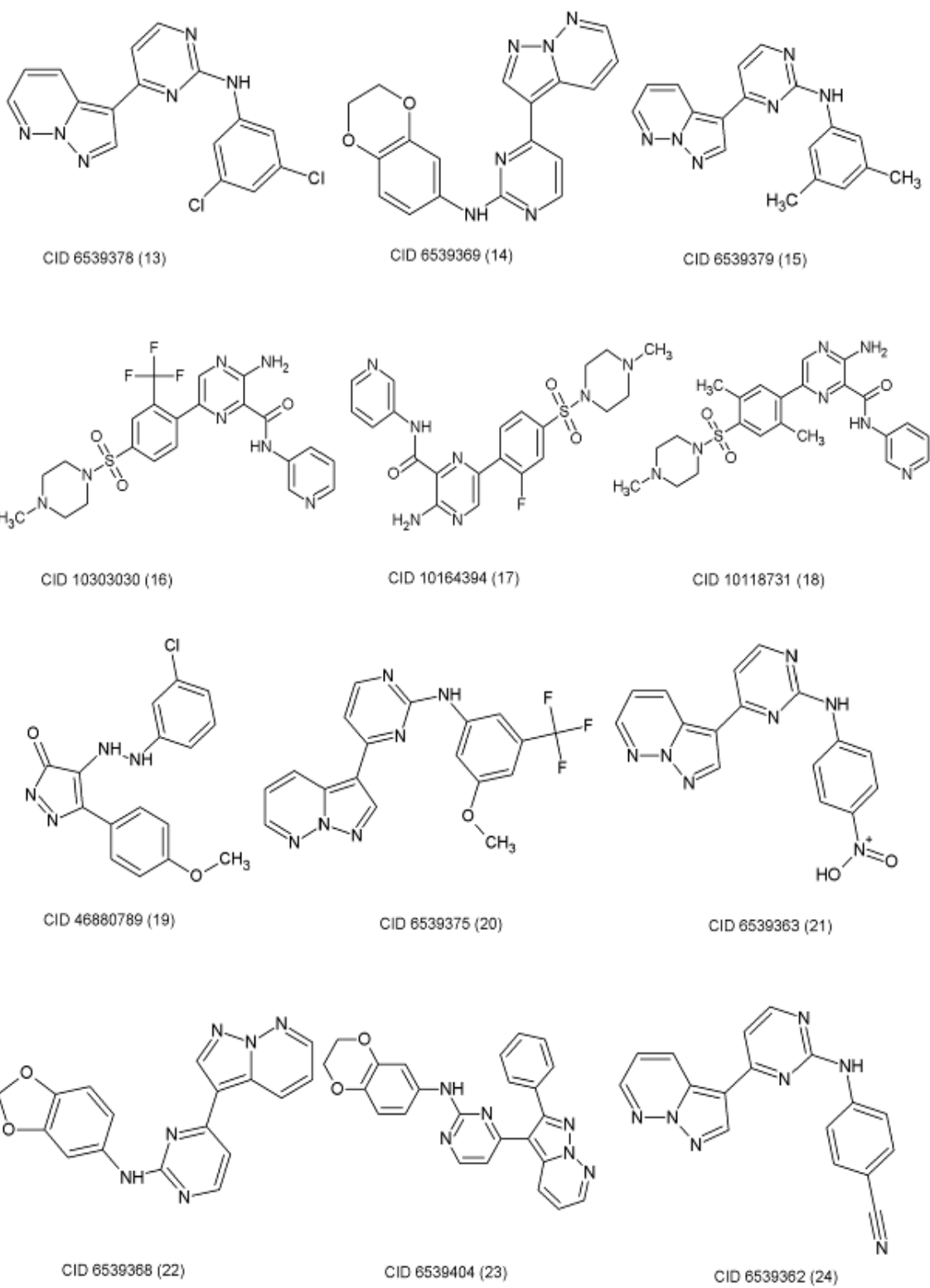


Fig. 1. Continuation

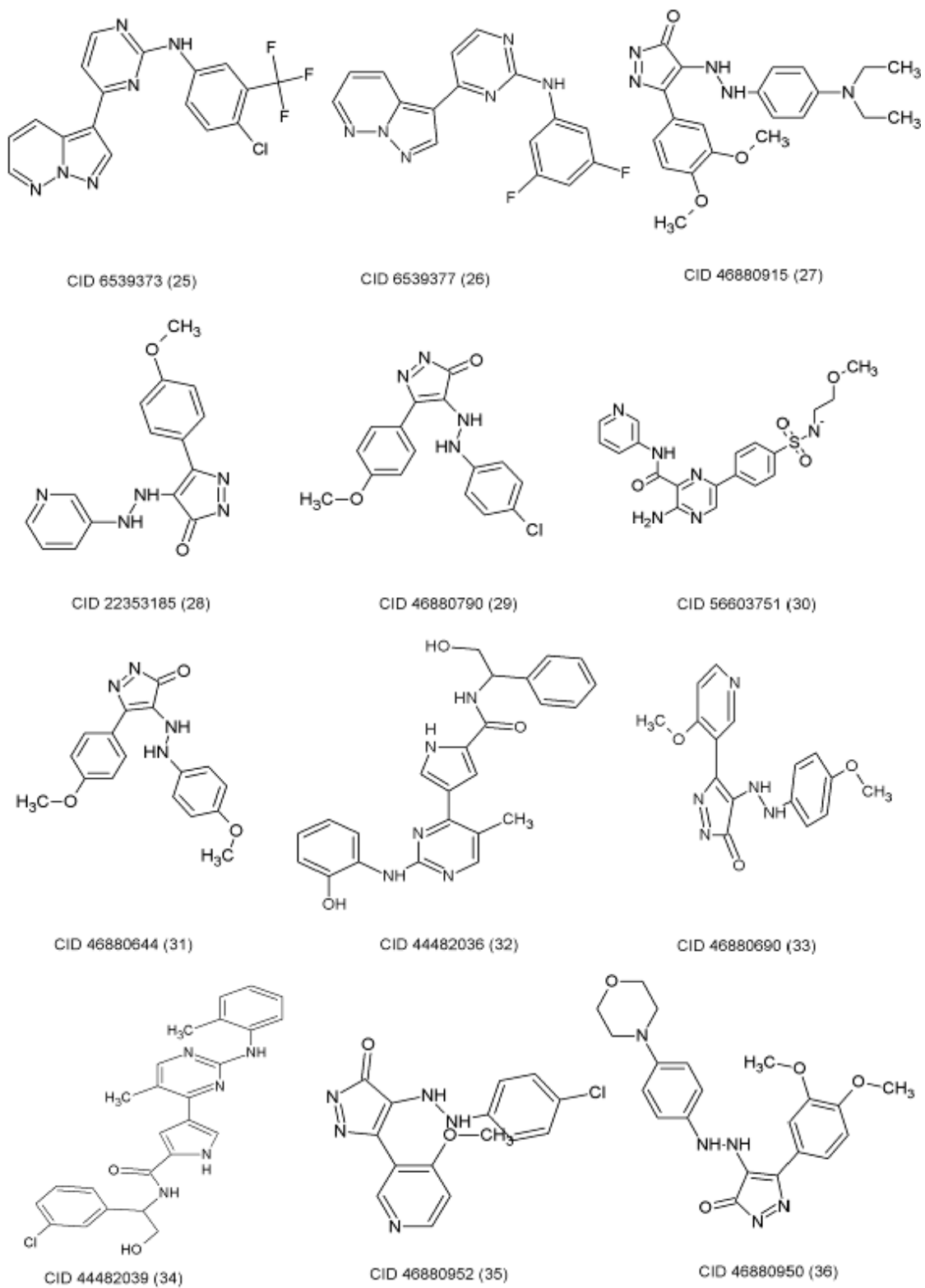
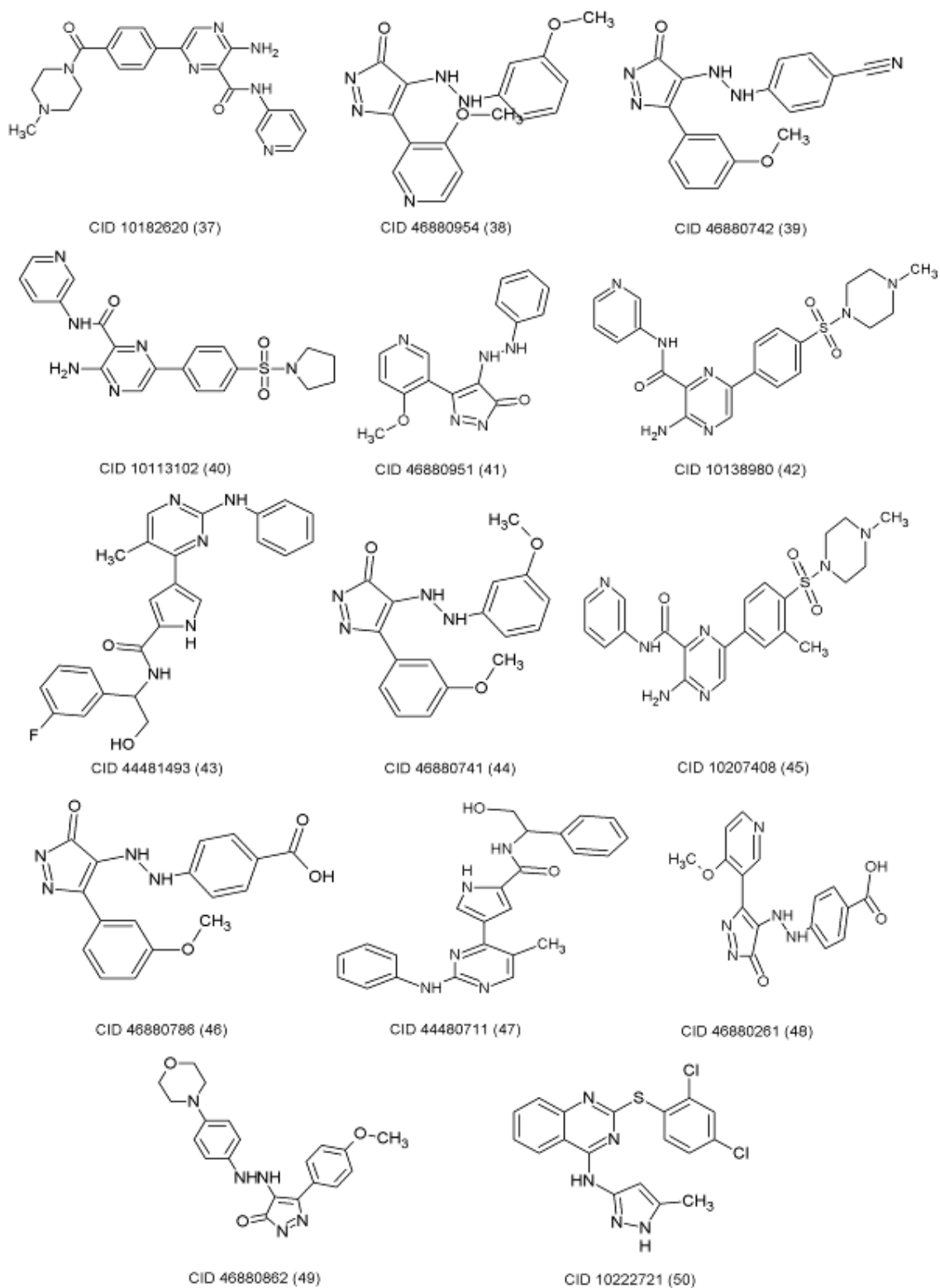


Fig. 1. Continuation



**Fig. 1. Inhibitors of GSK-3β identified in the database BindingDB**

**Table 1. Physicochemical parameters related to RO5 for selected GSK-3 $\beta$  inhibitors**

	<b>Inhibitor</b>	<b>Molecular weight (Dalton)</b>	<b>Hydrogen bond donor</b>	<b>Hydrogen bond acceptor</b>	<b>LogP</b>	<b>RO5 violations</b>	<b>Ki (nM)</b>
1	CID 9847557	471.30	3	8	4	0	0.09
2	CID 10231705	536.65	2	10	1	1	0.22
3	CID 6539376	435.20	1	8	4	0	0.3
4	CID 46880865	354.36	2	7	3.9	0	0.4
5	CID 46880864	358.78	2	6	4.5	0	0.4
6	CID 10138033	438.50	2	8	1.7	0	0.4
7	CID 10118014	467.54	2	9	1.1	0	0.46
8	CID 10142642	481.57	2	9	1.2	0	0.48
9	CID 10297008	440.48	2	9	0.5	0	0.67
10	CID 46865325	324.33	2	6	3.9	0	0.8
11	CID 71453604	460.53	2	11	0.9	1	0.99
12	CID 6539371	360.37	1	7	2.5	0	1
13	CID 6539378	357.20	1	5	3.7	0	1
14	CID 6539369	346.34	1	7	2.2	0	1
15	CID 6539379	316.36	1	5	3.2	0	1
16	CID 10303030	521.51	2	12	1.6	2	1.1
17	CID 10164394	471.51	2	10	0.8	0	1.3
18	CID 10118731	481.58	2	9	1.4	0	1.5
19	CID 46880789	328.75	2	5	4.5	0	1.9
20	CID 6539375	386.33	1	9	3.3	0	2
21	CID 6539363	333.30	1	7	2.3	0	2
22	CID 6539368	332.32	1	7	2.3	0	2
23	CID 6539404	422.44	1	7	3.8	0	2
24	CID 6539362	313.32	1	6	2.2	0	2
25	CID 6539373	390.74	1	8	4	0	2
26	CID 6539377	324.290	1	7	2.7	0	2
27	CID 46880915	395.45	2	7	4.7	0	2
28	CID 22353185	295.30	2	6	2.8	0	2
29	CID 46880790	328.75	2	5	4.5	0	2
30	CID 56603751	428.46	3	9	0.6	0	2
31	CID 46880644	324.33	2	6	3.9	0	2
32	CID 44482036	429.47	5	6	3	0	<2
33	CID 46880690	325.32	2	7	2.8	0	2
34	CID 44482039	461.94	4	5	4.3	0	<2
35	CID 46880952	329.74	2	6	3.5	0	3
36	CID 46880950	409.44	2	8	3.6	0	3
37	CID 10182620	417.46	2	7	1	0	3.1
38	CID 46880954	325.32	2	7	2.8	0	3.7
39	CID 46880742	319.32	2	6	3.6	0	4
40	CID 10113102	424.48	2	8	1.4	0	4.4
41	CID 46880951	295.30	2	6	2.8	0	4.5
42	CID 10138980	453.52	2	9	0.7	0	4.9
43	CID 44481493	431.46	4	6	3.4	0	5
44	CID 46880741	324.33	2	6	3.9	0	5
45	CID 10207408	467.54	2	9	1.1	0	6.3
46	CID46880786	338.32	3	7	3.4	0	6.5
47	CID 44480711	413.47	4	5	3.3	0	7
48	CID 46880261	339.30	3	8	2.4	0	7.7
49	CID 46880862	379.41	2	7	3.7	0	8
50	CID 10222721	402.30	2	5	6.1	1	80

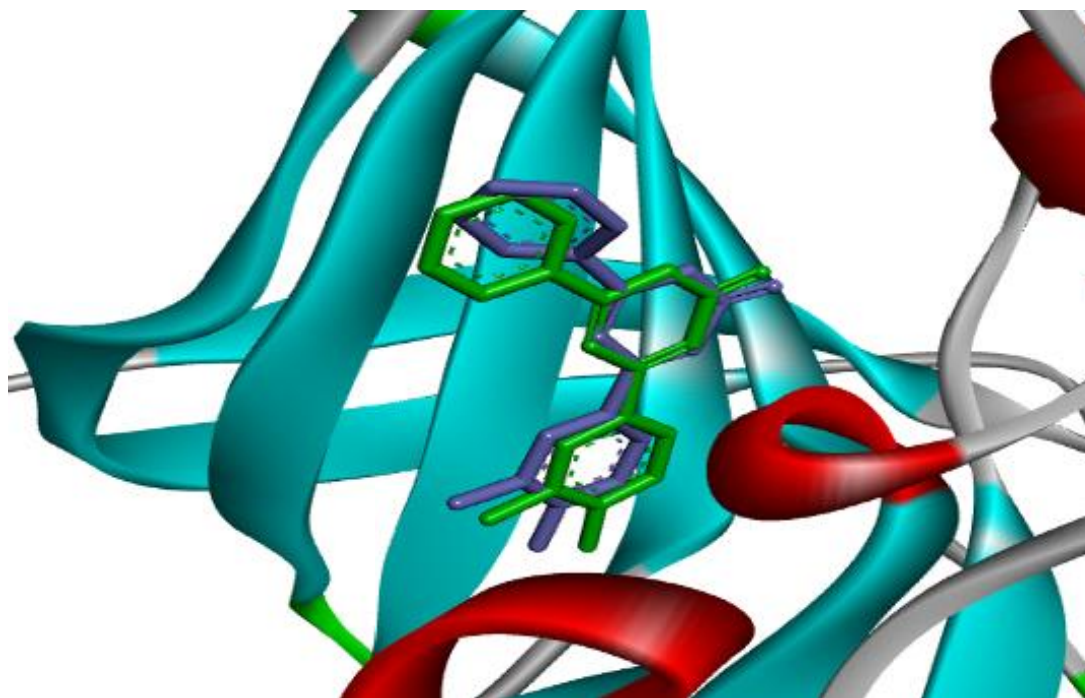


**Fig. 2. Reproduction of crystallographic pose of the inhibitor (green) inside the GSK-3 $\beta$  active site and the top-ranked docking solution (blue). Simulation was performed using the AutoDock Vina1.5.6 software**

Docking results point out hydrogen, ionic and hydrophobic interactions between ATP and Asp133, Tyr134, Val135, Pro136 and Arg141 residues of GSK-3 $\beta$  (PDB ID: 1Q5K) [38]. According Bidon-Chanal et al. [43] the GSK-3 $\beta$  inhibitor 'palinurin' performs ionic and hydrogen interactions with the Lys86 amino acid as well as a hydrogen bond with the Tyr56 residue.

32 molecules with higher inhibitory activity for GSK-3 $\beta$  were analyzed in the Pharmagist web-server for derivation of a common pharmacophoric pattern. In Figure 4 is observed the result with the highest score (55.701), respective to a set of 30 molecules aligned with four common pharmacophoric groups (or features): two aromatic rings and two hydrogen bond acceptors (pyrimidine group). Pharmacophore perception calculation can be used for predicting the biological effect of new drugs [30].

Pharmacophore is a summary of the description of the molecular features which are necessary for molecular recognition of a ligand by the macromolecule. These characteristics are

hydrophobic centers, aromatic rings, hydrogen bond acceptors, hydrogen bond donors, positive and negative ionizables [44]. Once identified, a pharmacophore can serve as a powerful model in the application of versatility for the rational design of drugs such as virtual screening studies and ADME/Tox [30,45].

According to Agrawal et al. [44] the best pharmacophoric pattern obtained for several GSK-3 inhibitors investigated were three aromatic rings, a hydrogen bond donor and a cation, with a score of 28.169 and t. Results obtained by Zidan et al. [15] using the PharmMapper approach, indicated that the pharmacophore model predicted for the tizoxanide, an active metabolite of nitazoxanide, has one donor and three hydrogen bond acceptors for binding GSK-3 $\beta$ .

According to Taha et al. [46] pharmacophore results for GSK-3 $\beta$  inhibitors corroborate this because they have hydrogen bond acceptors and aromatic rings as well as, in addition to hydrophobic and hydrogen bond donor groups.

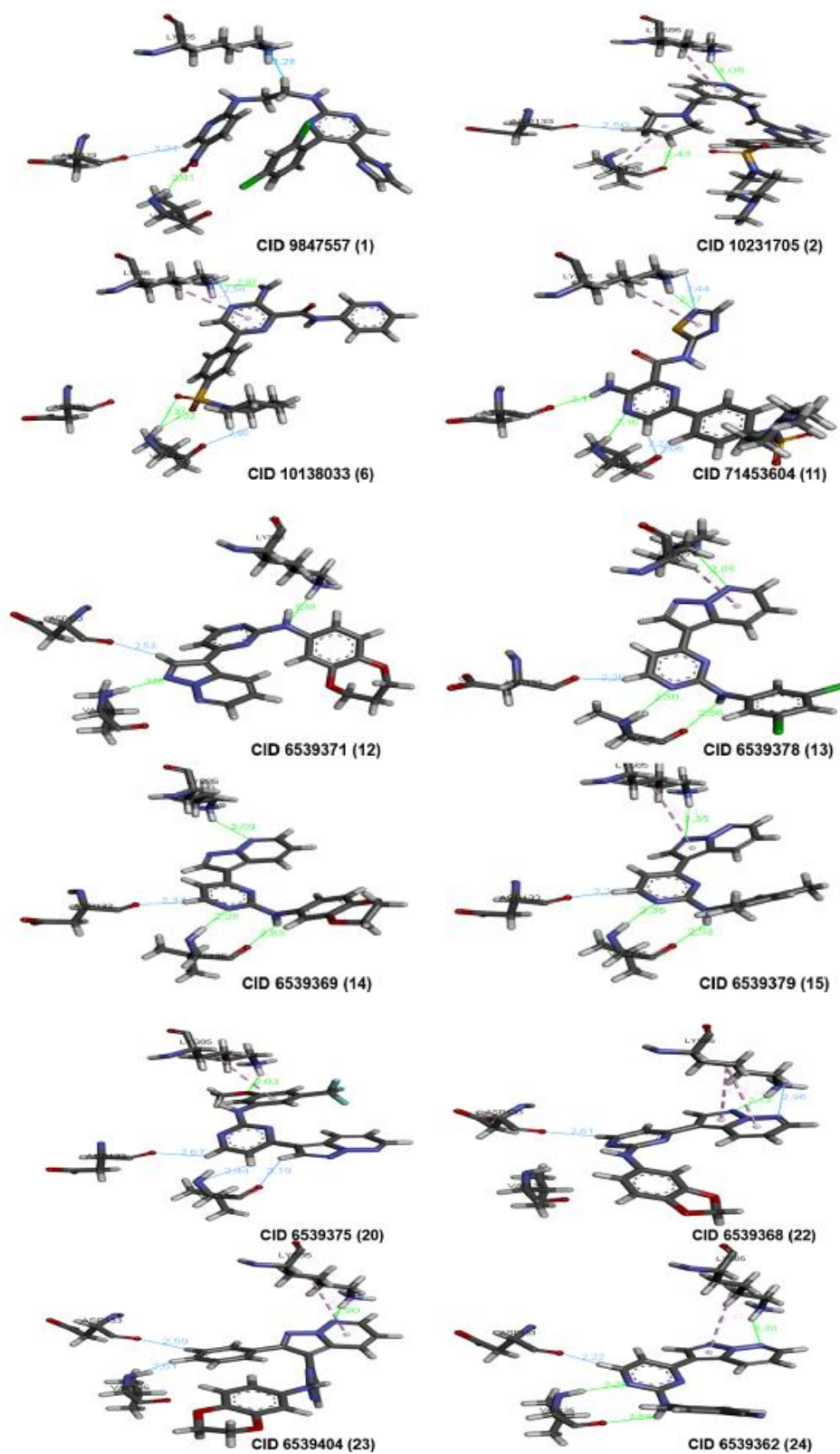
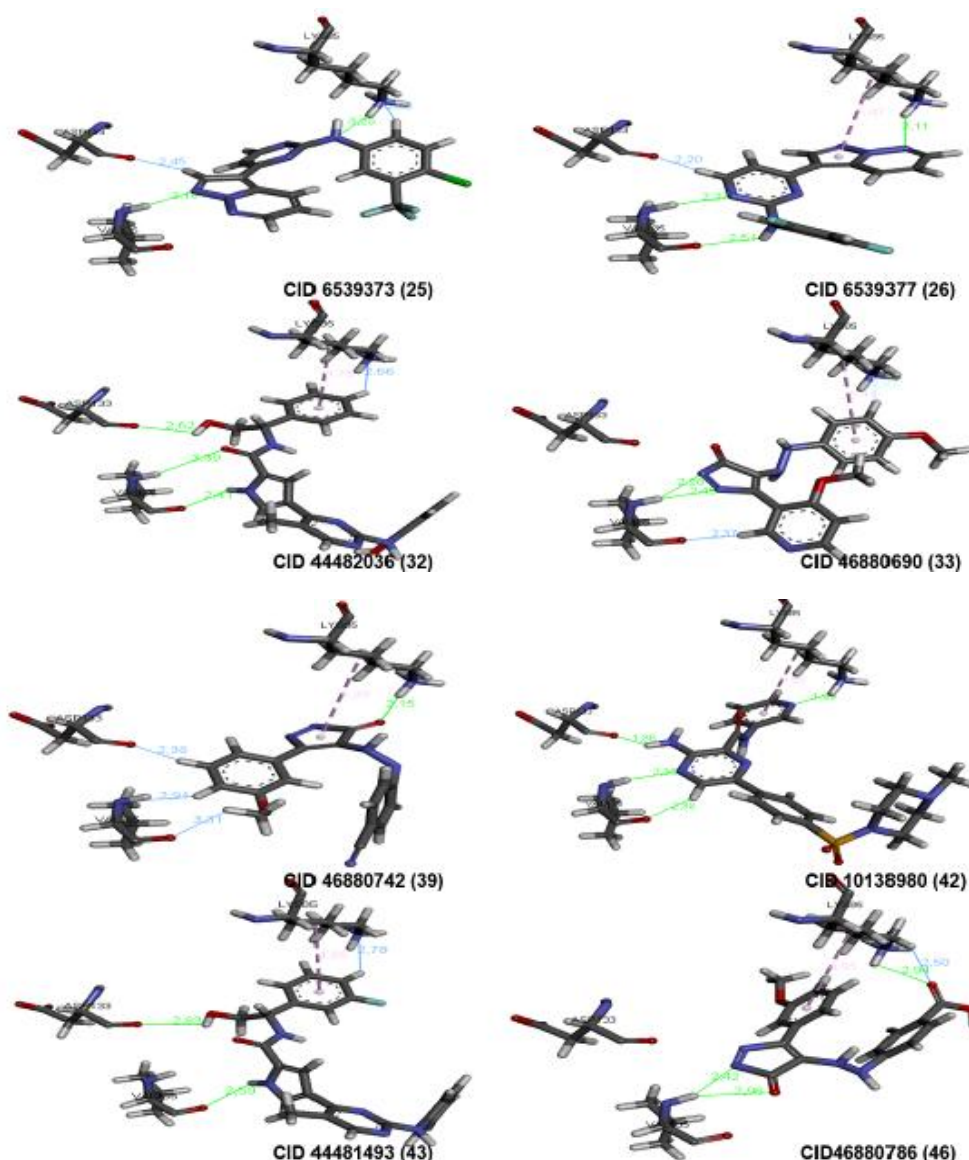


Fig. 3. Continuation



**Fig. 3. Top-ranked docking solutions for selected inhibitors and their interactions with the GSK-3 $\beta$  binding site: conventional hydrogen bonds (green), non-conventional hydrogen bonds (blue) and hydrophobic interactions (pink). Simulations were performed using the AutoDock Vina1.5.6 software**

The pharmacokinetic and toxicological predictions are essential for selection of drug candidates, because they allow the knowledge of ADME/Tox properties (absorption, distribution, metabolism, excretion and toxicity) to thereby facilitate modification or interruption of production of a drug if it has undesirable characteristics and provide a greater chance of success in the clinical trial stage [28,47,48].

Oral administration is the most used route due to its ease of accession. The drug is transported

into the stomach to the gastrointestinal tract [49,50]. In the analysis of human intestinal absorption were observed compounds with values in the range of  $88.0431 \leq \text{HIA} < 97.2448\%$ , that is, all the inhibitors are well absorbed, since they present values above the 20-70% range. According to Zhang et al. [51] the compound 2,3-Dihydro-2-benzyl-5-(2-nitrobenzyl)-1,5-benzothiazepine-4 (5H)-one, an potent GSK-3 $\beta$  inhibitor, shows a good intestinal absorption ability and capability of crossing the blood brain barrier BBB.

Caco-2 cells are well differentiated intestinal cells and derived from human colon adenocarcinoma, and exhibit morphological and functional characteristics similar to intestinal epithelium [52,53]. In a study of *in vitro* permeability of Caco-2 cells ( $P_{Caco2}$ ), the compounds showed an average permeability of 19.1808 nm / s. The obtained  $P_{Caco2}$  values are in the range of 6.024 to 31.611 nm / s, with the exception of the inhibitor 30 ( $P_{Caco2} = 0.8135$  nm / s), which presented a moderate permeability.

Madin-Darby canine Kidney (MDCK) cells are isolated from kidney tissue and differentiate into kidney cells in order to analyze its metabolism and transport [54,55]. According to the results of Table 3, it is observed that the inhibitors 5 ( $P_{MDCK}$

= 49.2847 nm / s), 10 ( $P_{MDCK} = 70.4439$  nm / s), 28 ( $P_{MDCK} = 37.6706$ ), 29 ( $P_{MDCK} = 42,5211$ nm / s), 39 ( $P_{MDCK} = 41.5282$  nm / s) and 44 ( $P_{MDCK} = 50.0467$  nm / s) have values in the range of 25-500 nm/s, in other words, have an average permeability in MDCK cells. The other compounds show low permeability ( $P_{MDCK} < 25$  nm / s) [56].

All selected compounds exhibited negative skin permeability values, thus showing no importance for transdermal administration (Table 4). The permeability of the skin is important for drugs that are administered transdermally, because it assesses the exposure of products that can cause tissue damage [57-59].

**Table 2. Top-ranked docking solutions and amino acids of the GSK-3 $\beta$  active site**

Analysis of the results of molecular docking generated using AutoDock Vina						
Compound	GSK-3 $\beta$ Inhibitors	Active site aminoacid	Atoms involved	Type of Interaction	Distance (Å)	Affinity (Kcal/mol)
1	CID 9847557	Lys85	H11 - NZ	Non-Conventional Hydrogen Bond	3.28	-8.7
		Asp133	H14 - O	Non-Conventional Hydrogen Bond	3.24	
		Val135	O4 - HN	Conventional Hydrogen Bond	2.01	
2	CID 10231705	Lys85	N9 - HZ3	Conventional Hydrogen Bond Hydrophobic	3.05 5.24	-9.1
		Asp133	H16 - O	Binding H non- conventional	2.50	
		Val135	H19 - O	Conventional Hydrogen Bond Hydrophobic	2.43 5.48	
6	CID 10138033	Lys85	H49 - NZ	Conventional Hydrogen Bond	2.97	-8.4
		Lys85	N7 - HE2	Non-Conventional Hydrogen Bond Hydrophobic	2.54 5.15	
		Asp133	-	-	-	
		Val135	O2 - HN	Conventional Hydrogen Bond	2.97	
		Val135	O3 - HN	Conventional Hydrogen Bond	2.32	
11	CID 71453604	Lys85	H12 - O	Non-Conventional Hydrogen Bond	2.98	-8.7
		Lys85	N13 - HZ1	Non-Conventional Hydrogen Bond	3.44	
		Lys85	N13 - HZ3	Conventional Hydrogen Bond Hydrophobic	2.27 4.97	
		Asp133	H49 - O	Conventional Hydrogen Bond	2.17	
		Val135	N9 - HN	Conventional	2.16	

Analysis of the results of molecular docking generated using AutoDock Vina									
Compound	GSK-3 $\beta$ Inhibitors	Active site aminoacid	Atoms involved	Type of Interaction	Distance (Å)	Affinity (Kcal/mol)			
12	CID 6539371	Val135	H8 - O	Hydrogen Bond	2.27	-9.1			
				Non-Conventional Hydrogen Bond					
				Hydrogen Bond					
		Lys85	N3 - HZ3	Conventional Hydrogen Bond	3.38				
				Asp133			H18 - O	Non-Conventional Hydrogen Bond	2.53
								Val135	
13	CID 6539378	Lys85	N7 - HZ3	Conventional Hydrogen Bond	2.88	-8.5			
				Hydrogen Bond					
				Hydrophobic			5.43		
		Asp133	H6 - O	Non-Conventional Hydrogen Bond	2.20				
				Val135			N8 - HN	Conventional Hydrogen Bond	2.30
								H28 - O	
14	CID 6539369	Lys85	N7 - HZ3	Conventional Hydrogen Bond	3.09	-8.9			
				Hydrogen Bond					
				Hydrophobic			5.43		
		Asp133	H10 - O	Non-Conventional Hydrogen Bond	2.37				
				Val135			N8 - HN	Conventional Hydrogen Bond	2.28
								H34 - O	
15	CID 6539379	Lys85	N4 - HZ3	Conventional Hydrogen Bond	3.35	-8.6			
				Hydrogen Bond					
				Hydrophobic			5.44		
		Asp133	H6 - O	Non-Conventional Hydrogen Bond	2.26				
				Val135			N6 - HN	Conventional Hydrogen Bond	2.36
								H29 - O	
20	CID 6539375	Lys85	O4 - HZ3	Conventional Hydrogen Bond	2.03	-8.9			
				Hydrogen Bond					
				Hydrophobic			4.81		
		Asp133	H6 - O	Non-Conventional Hydrogen Bond	2.67				
				Val135			H5 - N	Non-Conventional Hydrogen Bond	2.94
								H7 - O	
22	CID 6539368	Lys85	N6 - HZ3	Hydrophobic	4.57	-9.1			
				Hydrophobic			5.16		
				Conventional Hydrogen Bond			2.12		
		Asp133	H8 - O	Non-Conventional Hydrogen Bond	2.96				
				Val135			N7 - NZ	Non-Conventional Hydrogen Bond	2.96
								H8 - O	

Analysis of the results of molecular docking generated using AutoDock Vina						
Compound	GSK-3 $\beta$ Inhibitors	Active site aminoacid	Atoms involved	Type of Interaction	Distance (Å)	Affinity (Kcal/mol)
23	CID 6539404	Lys85	N7 - HZ3	Hydrogen Bond	-	-9.9
				Conventional Hydrogen Bond	2.90	
				Hydrophobic	5.35	
				Non-Conventional Hydrogen Bond	2.59	
				Non-Conventional Hydrogen Bond	2.51	
24	CID 6539362	Lys85	N5 - HZ3	Conventional Hydrogen Bond	3.33	-8.5
				Hydrophobic	5.47	
				Non-Conventional Hydrogen Bond	2.22	
				Conventional Hydrogen Bond	2.38	
				Conventional Hydrogen Bond	2.59	
25	CID 6539373	Lys85	H3 - NZ	Non-Conventional Hydrogen Bond	2.93	-8.7
				Conventional Hydrogen Bond	3.25	
				Non-Conventional Hydrogen Bond	2.45	
				Conventional Hydrogen Bond	2.10	
				Conventional Hydrogen Bond	2.10	
26	CID 6539377	Lys85	N7 - HZ3	Conventional Hydrogen Bond	3.11	-8.5
				Hydrophobic	5.47	
				Non-Conventional Hydrogen Bond	2.20	
				Conventional Hydrogen Bond	2.27	
				Conventional Hydrogen Bond	2.51	
32	CID 44482036	Lys85	H11 - NZ	Non-Conventional Hydrogen Bond	2.66	-8.4
				Hydrophobic	4.75	
				Conventional Hydrogen Bond	2.62	
				Conventional Hydrogen Bond	3.39	
				Conventional Hydrogen Bond	2.41	
33	CID 46880690	Lys85	H11 - NZ	Non-Conventional Hydrogen Bond	2.87	-7.2
				Hydrophobic	5.41	
				Conventional Hydrogen Bond	2.28	
				Conventional Hydrogen Bond	2.45	
				Non-Conventional Hydrogen Bond	2.35	
39			O2 - HZ3	Conventional	2.15	

Analysis of the results of molecular docking generated using AutoDock Vina								
Compound	GSK-3β Inhibitors	Active site aminoacid	Atoms involved	Type of Interaction	Distance (Å)	Affinity (Kcal/mol)		
42	CID 46880742	Lys85		Hydrogen Bond	5.35	-7.9		
				Hydrophobic				
		Asp133	H7 - O	Non-Conventional Hydrogen Bond	2.38			
		Val135	H6 - N	Non-Conventional Hydrogen Bond	2.91			
H4 - O	Non-Conventional Hydrogen Bond		3.31					
42	CID 10138980	Lys85	N11 - HZ3	Conventional Hydrogen Bond	1.99	-8.3		
				Hydrophobic	4.89			
		Asp133	H51 - O	Conventional Hydrogen Bond	1.86			
		Val135	N8 - HN	Conventional Hydrogen Bond	2.35			
H8 - O	Conventional Hydrogen Bond		2.38					
43	CID 44481493	Lys85	H8 - NZ	Non-Conventional Hydrogen Bond	2.78	-8.5		
				Hydrophobic	4.88			
				Asp133	H48 - O		Conventional Hydrogen Bond	2.83
46	CID46880 786	Val135	H38 - O	Conventional Hydrogen Bond	2.59	-8.0		
				O4 - HE2	Non-Conventional Hydrogen Bond		2.50	
				Lys85	O4 - HZ3		Conventional Hydrogen Bond	2.94
				Hydrophobic	4.95			
48	CID 46880261	Val135	H11 - O	Conventional Hydrogen Bond	2.42	-7.5		
				O2- HN	Conventional Hydrogen Bond		2.96	
				N8 - HZ3	Conventional Hydrogen Bond		2.15	
				Hydrophobic	4.95			
50	CID 10222721	Val135	H69 - OE1	Non-Conventional Hydrogen Bond	3.31	-8.8		
				Hydrophobic	3.25			
				Hydrogen Bond	2.75			
				Hydrogen Bond	3.25			
				Hydrogen Bond	3.25			
50	CID 10222721	Lys85		Non-Conventional Hydrogen Bond	3.01	-8.8		
				Hydrophobic	4.64			
				Hydrophobic	4.64			
				Conventional Hydrogen Bond	1.96			
				Conventional Hydrogen Bond	1.96			

**Table 3. Absorption properties of GSK-3 $\beta$  inhibitors**

	<b>Compound</b>	<b>P<sub>Caco2</sub> (nm/sec)</b>	<b>P<sub>MDCK</sub> (nm/sec)</b>	<b>HIA (%)</b>	<b>P<sub>Skin</sub> (cm/hora)</b>
1	CID 9847557	14.809	0.05834	89.4912	-3.89663
2	CID 10231705	21.261	0.37748	97.0905	-3.97818
3	CID 6539376	26.519	0.03716	96.5848	-2.21353
4	CID 46880865	23.355	24.03960	94.1093	-3.81971
5	CID 46880864	21.126	49.28470	94.3231	-3.70158
6	CID 10138033	18.583	2.14435	96.0189	-3.71335
7	CID 10118014	20.316	0.75513	96.1520	-3.83193
8	CID 10142642	20.773	1.84285	96.4837	-3.74530
9	CID 10297008	17.836	0.45171	94.0572	-4.13202
10	CID 46865325	22.445	70.44390	93.7571	-3.69334
11	CID 71453604	8.212	0.41950	85.3501	-4.34007
12	CID 6539371	11.637	4.13720	96.8768	-4.15107
13	CID 6539378	24.047	0.10729	96.6258	-3.30302
14	CID 6539369	9.2059	6.22295	96.9313	-4.18593
15	CID 6539379	30.183	0.11376	96.0690	-3.19497
16	CID 10303030	17.555	0.24295	96.2260	-2.91327
17	CID 10164394	19.660	2.04905	95.7820	-4.16225
18	CID 10118731	20.605	0.17929	96.4841	-3.68794
19	CID 46880789	20.983	137.29800	94.1976	-3.58055
20	CID 6539375	21.812	0.05560	96.3706	-2.49487
21	CID 6539363	20.641	7.59235	94.9151	-3.48538
22	CID 6539368	12.669	15.14160	96.9861	-4.21156
23	CID 6539404	24.764	0.21666	96.5817	-3.38178
24	CID 6539362	20.139	16.38620	97.2448	-3.27016
25	CID 6539373	24.588	0.05104	96.3183	-2.28155
26	CID 6539377	17.821	0.30354	96.0206	-3.78144
27	CID 46880915	31.611	0.07369	94.3632	-3.45415
28	CID 22353185	20.881	37.67060	93.3997	-4.12799
29	CID 46880790	20.019	42.52110	94.1976	-3.58941
30	CID 56603751	0.8135	0.38946	89.2699	-3.60544
31	CID 46880644	21.503	3.96466	93.7571	-3.69805
32	CID 44482036	19.789	0.18936	82.6947	-3.67888
33	CID 46880690	6.024	15.31330	93.3871	-4.17426
34	CID 44482039	21.953	0.30500	90.4022	-3.47768
35	CID 46880952	19.188	5.05744	94.1722	-4.08405
36	CID 46880950	27.015	0.54283	94.6259	-4.10079
37	CID 10182620	20.775	1.19025	95.8886	-4.20800
38	CID 46880954	20.255	6.23448	93.3871	-4.17014
39	CID 46880742	15.846	41.52820	93.9270	-3.54095
40	CID 10113102	16.560	2.35626	95.6161	-3.90891
41	CID 46880951	9.344	6.65281	93.4010	-4.09381
42	CID 10138980	19.971	1.10342	95.7527	-3.93860
43	CID 44481493	22.958	0.22342	88.0769	-3.79879
44	CID 46880741	21.699	50.04670	93.7571	-3.6899
45	CID 10207408	20.349	0.59563	96.1520	-3.83591
46	CID 46880786	19.332	2.12502	91.0401	-3.80477
47	CID 44480711	22.396	1.83088	88.0431	-3.49959
48	CID 46880261	18.212	21.85790	84.1103	-4.26337
49	CID 46880862	26.134	0.38737	94.2718	-3.96850
50	CID 10222721	24.885	0.12966	94.3380	-3.41641

$P_{Caco2}$  = Caco2 Cell Permeability;  $P_{MDCK}$  = MDCK Cell Permeability; HIA = Human Intestinal Absorption;  $P_{Skin}$  = Skin Permeability

**Table 4. Property of distribution in LPP percentages and BBB penetration for the GSK-3 $\beta$  inhibitors investigated**

	<b>Compound</b>	<b>BBB [Brain]/[Blood]</b>	<b>PPB (%)</b>
1	CID 9847557	0.136004	92.0608
2	CID 10231705	0.0645645	13.1861
3	CID 6539376	0.127831	100
4	CID 46880865	0.0292765	80.6802
5	CID 46880864	0.110631	88.068
6	CID 10138033	0.0785441	75.0897
7	CID 10118014	0.0645104	35.3233
8	CID 10142642	0.0683089	34.9866
9	CID 10297008	0.0526544	62.0253
10	CID 46865325	0.0621524	84.2758
11	CID 71453604	0.0463356	31.0749
12	CID 6539371	0.359008	86.4131
13	CID 6539378	0.179928	95.316
14	CID 6539369	0.326015	86.3556
15	CID 6539379	0.255073	90.2344
16	CID 10303030	0.0740106	79.63
17	CID 10164394	0.0606371	28.3218
18	CID 10118731	0.0750119	38.0732
19	CID 46880789	0.37966	90.9626
20	CID 6539375	0.0380007	88.5134
21	CID 6539363	0.176305	91.1206
22	CID 6539368	0.311313	86.9634
23	CID 6539404	0.466094	90.0879
24	CID 6539362	0.358618	96.3473
25	CID 6539373	0.112118	90.1621
26	CID 6539377	0.114434	90.1456
27	CID 46880915	0.0964415	86.4156
28	CID 22353185	0.0162709	60.2541
29	CID 46880790	0.274524	92.3967
30	CID 56603751	0.0551824	59.4904
31	CID 46880644	0.0482028	84.0441
32	CID 44482036	0.358346	90.9979
33	CID 46880690	0.0131923	75.4786
34	CID 44482039	2.07304	90.4415
35	CID 46880952	0.0213406	86.9236
36	CID 46880950	0.0267125	78.6572
37	CID 10182620	0.0700923	29.921
38	CID 46880954	0.0574268	75.0722
39	CID 46880742	0.0192447	82.1933
40	CID 10113102	0.0678396	69.7952
41	CID 46880951	0.0196721	77.6022
42	CID 10138980	0.0576161	31.283
43	CID 44481493	0.950117	89.0312
44	CID 46880741	0.0456664	83.757
45	CID 10207408	0.0653221	33.1416
46	CID 46880786	0.0444779	79.6958
47	CID 44480711	0.813774	97.0318
48	CID 46880261	0.0584119	66.7854
49	CID 46880862	0.0376162	85.7063
50	CID 10222721	4.69306	87.1054

*BBB = Blood-Brain Barrier; PPB = Plasma Protein Binding*

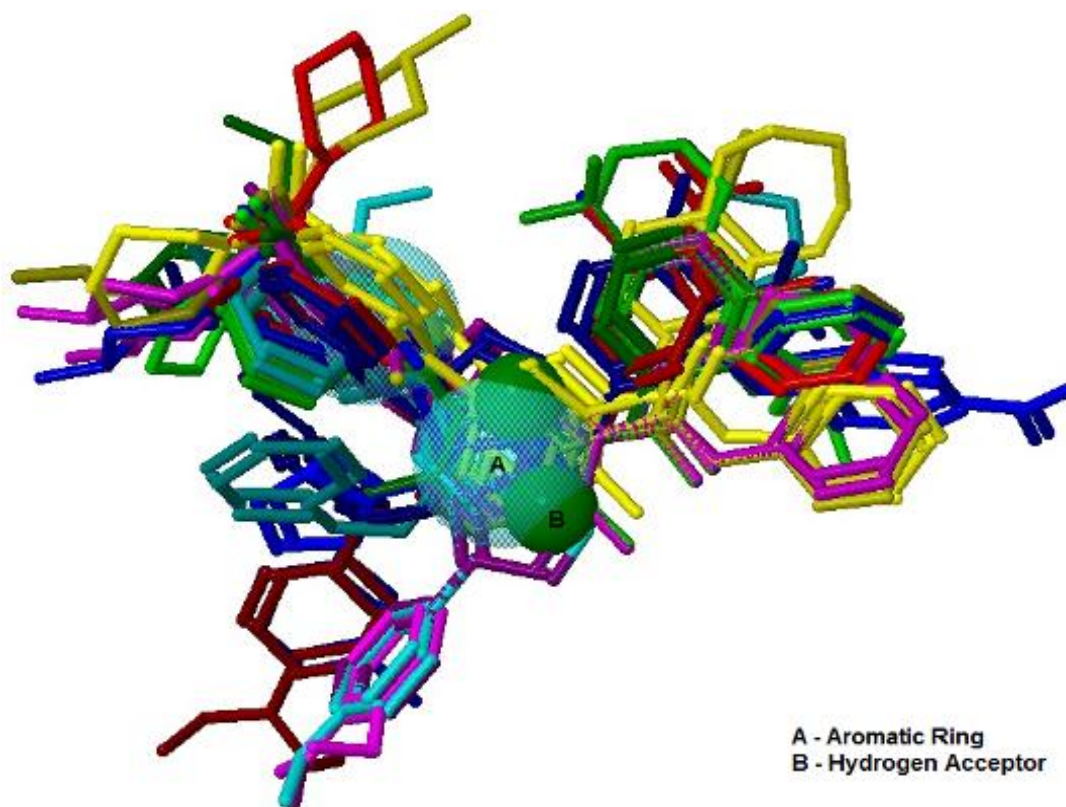


**Fig. 4.** Best pharmacophore model generated by alignment of 30 GSK-3 $\beta$  inhibitors, using the PharmaGist web server

The binding of a drug to plasma proteins is due to van der Waals interactions and hydrogen bonding, so this binding is reversible, which influences in the delivery of the drug by the body. When a drug binds strongly to these proteins its therapeutic effect is lower because there is a small fraction of the drug free to cross the membranes [60-62].

In Table 3, concerning the binding property of plasma proteins, inhibitors 2 (PPB = 13.1861%), 4 (PPB = 80.6802%), 5 (PPB = 88.068%), 6 (= 75.0897% PPB), 7 (PPB = 35.3233%), 8 (PPB = 34.9866%), 9 (PPB = 62.0253%), 10 (PPB = 84.2758%), 11 (PPB = 31.0749%), 12 (PPB = 86.4131%), 14 (PPB = 86.3556%), 16 (PPB = 79.63%), 17 (PPB = 28.3218%), 18 (PPB = 38.0732%), 20 (PPB = 88.5134%), 22 (PPB = 86.9634%), 27 (PPB = 86.4156%), 28 (PPB = 60.2541%), 30 (PPB = 59.4904%), 31 (PPB = 84.0441%), 33 (PPB = 75.4786%), 35 (PPB = 86.9236%), 36 (PPB = 78.6572%), 37 (PPB = 29.921%), 38 (PPB = 75.0722%) and 39 (= 82 PPB 1933%), 40 (PPB = 69.7952%), 41 (PPB =

77.6022%), 42 (PPB = 31.283%), 43 (PPB = 89.0312%), 44 (PPB = 83.757%) 45 (PPB = 33.1416%), 46 (PPB = 79.6958%), 48 (PPB = 66.7854%), 49 (PPB = 85.7063%) and 50 (PPB = 87.1054%) weakly bind plasma proteins (PPB < 90%), presenting a variation from 13.1861% to 89.0312%.

Table 4 shows the amount of penetration in the BBB MA et al. [63] classification, where compounds which have values  $C_{\text{brain}}/C_{\text{blood}} > 1$  are able to cross the BBB and compounds with values below 1 do not act on the central nervous system. In analyzing the results, the inhibitors 34 ( $C_{\text{brain}}/C_{\text{blood}} = 2.07304$ ) and 50 ( $C_{\text{brain}}/C_{\text{blood}} = 4.69306$ ) are able to cross the BBB, but theoretically they do not act on the central nervous system, showing an average value of  $C_{\text{brain}}/C_{\text{blood}} = 0.283102164$ . BBB consists in a biological membrane comprised of endothelial cells, metabolic enzymes and transport proteins, which maintains brain homeostasis, as preventing entry of endogenous substances that may be toxic [64-66].

In order to propose novel GSK-3 $\beta$  inhibitors candidates with drug-like properties, we have used compound 1 (CID 9847557) as a prototype (Fig. 5) due to its high inhibitory activity ( $K_i = 0.09$ ), its affinity with GSK-3 $\beta$  (interactions with Lys = 3, at 2.8 Å, Asp133 and Val135, at = 3.24 and 2.01 Å, respectively) and because it has groups common to the pharmacophoric pattern here calculated (two aromatic rings and two hydrogen bond acceptors).

In order to reduce the molecular weight and increase lipophilicity, the imidazole group has been removed from the prototype CID 9847557 (Proposal 1), as these properties play a key role for crossing the BBB. In the second proposal, the aminoethyl side chain was removed, also aiming to reduce the molecular weight. In the proposal 3, it is observed the addition of the hydroxyl group (OH) at the C32 position of the pyridine ring, in order to increase the interaction with Asp133 of the GSK-3 $\beta$  active site (Fig. 6).

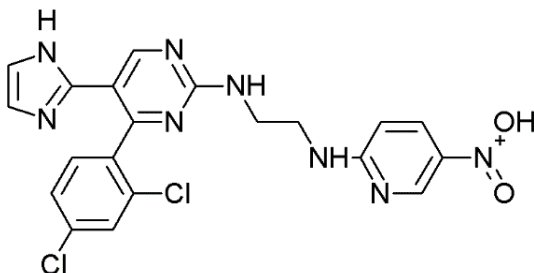


**Fig. 5. Prototype CID 9847557**

The *in silico* prediction of activity spectra of the substances (PASS) provides whether a drug candidate is active against a biological target based on physicochemical methods using

different algorithms and comparisons. The biological activities are: pharmacological and side effects, mechanism of action, mutagenicity, carcinogenicity, teratogenicity and embryotoxicity [35,67].

In the outcome of the prediction of biological activity, the activities with the value of  $P_a > P_i$  were considered, where  $P_a$  = probability to be active and  $P_i$  = probability to be inactive, and the values range from 0 to 1. The following table shows the values obtained for the 3 proposals of GSK-3 $\beta$  inhibitors candidates. The three proposals had  $P_a > P_i$  values (Table 5) (Proposal 1:  $P_a = 0.120$ ; Proposal 2: 0.242; Proposal 3: 0.139), thus indicating biological activity for GSK-3 $\beta$ . However, according Lagunin et al. [68] when the value of  $P_a$  is less than 0.5, it becomes unlikely that the substance exhibits an experimental activity. On the other hand, if the presence is confirmed in experiments, then the substance can be considered a new chemical entity.

**Table 5. Prediction of biological activity for GSK-3 $\beta$  inhibitors candidates**

Compound	$P_a$	$P_i$
Proposal 1	0.120	0.028
Proposal 2	0.242	0.006
Proposal 3	0.139	0.020

Finally, after prediction of biological activity, we calculated synthetic accessibility for all the proposals, using the SYLVIA software [34]. All the proposals indicate medium synthetic accessibility structures, according the rules/parameters of such algorithm (Proposal 1 = 3.93; Proposal 2 = 4.15 and Proposal 3 = 4.39).

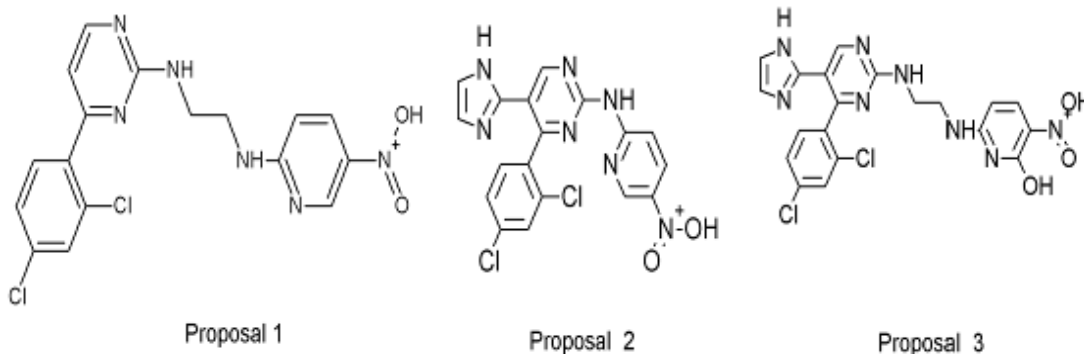


**Fig. 6. Proposals of candidates for GSK-3 $\beta$  inhibitors**

#### 4. CONCLUSION

In silico calculations were here performed to propose new GSK-3 $\beta$  inhibitors candidates, with drug-like properties. We have carried out docking simulation, ADME prediction, pharmacophore perception and analysis of physicochemical parameters for selected inhibitors reported in literature. Most of the compounds showed no more than two violations to the rule of five, with a good oral availability. Docking results indicate 22 inhibitors with strong interactions with the amino acid residues of the enzyme active site (hydrogen bond and hydrophobic interactions).

For pharmacophore perception calculation, 30 molecules were superimposed with four pharmacophore groups: two aromatic rings and two hydrogen bond acceptors (pyrimidine group). In ADME prediction, most inhibitors show good permeability for both Caco2 and MDCK cells, high intestine absorption and weak binding to plasma proteins, but only inhibitors 34 and 50 show ability for crossing the BBB, which is essential for the action in CNS. The three proposals for novel GSK-3 $\beta$  inhibitors here investigated show potential biological activity for GSK-3 $\beta$ , as well as having medium synthetic accessibility. Therefore, additional quantitative structure-activity relationship studies are needed to investigate how the chemical structures of these molecules affect its biological potency and binding affinity with GSK-3 $\beta$  enzyme, as a guide to optimize these potential drug candidates here proposed for future AD treatment.

#### CONSENT

It is not applicable.

#### ETHICAL APPROVAL

It is not applicable.

#### COMPETING INTERESTS

Authors have declared that no competing interests exist.

#### REFERENCES

1. Muchowski PJ, Wacker JL. Modulation of neurodegeneration by molecular chaperones. *Nat Rev Neurosci.* 2005;6(1): 11-22.
2. Sequeira ACR. Efeitos neuroprotetores das sirtuínas – Potencial intervenção terapêutica em doenças neurodegenerativas. Dissertação (Mestrado em Medicina), Faculdade de Medicina da Universidade do Porto, Porto; 2012. Portuguese.
3. Querfurth HW, Laferla, FM. Alzheimer's disease. *N Engl J Med.* 2010;362:329–44.
4. Vieira LCC. Síntese de uma coleção de cumarinas, possíveis inibidores da enzima acetilcolinesterase. Dissertação (Mestrado em Química), Universidade Federal de São Carlos, São Carlos; 2010. Portuguese.
5. Acosta-Baena N, Sepulveda-Falla D, Lopera-Gómez CM, Jaramillo-Elorza MC, Moreno S, Aguirre-Acevedo DC, Saldarriaga A, Lopera F. Pre-dementia clinical stages in presenilin 1 E280A familial early-onset Alzheimer's disease: A retrospective cohort study. *Lancet Neurol.* 2011;10(3):213–220.
6. Moser DA. Mal de Alzheimer na primeira fase: contribuições da psicolinguística. Tese (Doutorado em Linguística - Psicolinguística), Universidade Federal de Santa Catarina, Florianópolis; 2011. Portuguese.
7. Brandt R, Hanser H. O enigma de Alzheimer. In: Ferrari AC, Zeni B. (Eds.). *Viver mente & cérebro.* São Paulo:Duetto. 2004;142:68-73.
8. Botelho L. Alzheimer: A doença da alma. Campinas: Russell Editores; 2008.
9. Citron M. Strategies for disease modification in Alzheimer's disease. *Nat Rev Neurosci.* 2004;5:677-685.
10. Fridman C, Gregório SP, Ojopi ÉPB, Dias Neto E. Alterações genéticas na doença de Alzheimer. *Rev Psiq Clín.* 2004;31(1): 19-25.
11. De Melo GO, Costa SS. Produtos Naturais para o tratamento da doença de Alzheimer: Promessa e Desafio. *Rev Fito.* 2005;1(2):41-47.
12. Lee G, Leugers CJ. Tau and Tauopathies. *Prog Mol Bio Transl Sci.* 2012;107:263-293.
13. Vieira TS. Estudos visando à síntese de novos derivados do LCC com potencial atividade no tratamento da doença de Alzheimer. Dissertação (Mestrado em Química), Universidade de Brasília, Brasília; 2007. Portuguese.

14. Neto JG, Tamelini MG, Forlenza OV. Diagnóstico diferencial das demências. *Rev Psiq Clín.* 2005;32(3):119-130.
15. Zidan M, Arcoverde C, Araújo NB, Vasques P, Rios A, Laks J, Deslandes A. Alterações motoras e funcionais em diferentes estágios da doença de Alzheimer. *Rev Psiq Clín.* 2012;39(5):161-165.
16. Greenlee W, Clader J, Asberom T, McCombie S, Ford J, Guzik H, Kozlowski J, Li S, Liu C, Lowe D, Vice S, Zhao H, Zhou G, Billard W, Binch H, Crosby R, Duffy R, Lachowicz J, Coffin V, Watkins R, Ruperto V, Strader C, Taylor L, Cox K.. Muscarinic agonists and antagonists in the treatment of Alzheimer's disease. *Farmacologia.* 2001; 56:247.
17. Cerqueira AAB. Estratégias farmacológicas para as alterações precoces do comportamento na doença de Alzheimer. Dissertação (Mestrado em Medicina), Universidade de Coimbra, Coimbra; 2009. Portuguese.
18. Hardt SE, Sadoshima J. Glycogen synthase kinase-3beta: A novel regulator of cardiac hypertrophy and development. *Circ Res.* 2002;90:1055-1063.
19. Doble BW, Woodgett Jr. GSK-3: tricks of the trade for a multi-tasking kinase. *J Cell Sci.* 2003;1(116):1175-86.
20. Le Corre M, Carey Susan. One, two, three, four, nothing more: An investigation of the conceptual sources of the verbal counting principles. *Cognition.* 2007;105(2):395-438.
21. Hernandez L, Roux KJ, Wong ES, Mounkes LC, Mutalif R, Navasankari R, Rai B, Cool S, Jeong JW, Wang H, Lee HS, Kozlov S, Grunert M, Keeble T, Jones CM, Meta MD, Young SG, Daar IO, Burke B, Perantoni AO, Stewart CL. Functional coupling between the extracellular matrix and nuclear lamina by Wnt signaling in progeria. *Dev Cell.* 2010;19(3):413-25.
22. Leroy X, Aubert S, Zini L, Franquet H, Kervoaze G, Villers A, Delehedde M, Copin MC, Lassalle P. Vascular endocan (ESM-1) is markedly overexpressed in clear cell renal cell carcinoma. *Histopathology.* 2010;56(2):180-187
23. Cramer PE, Cirrito JR, Wesson DW, Lee CY, Karlo JC, Zinn AE, Casali BT, Restivo JL, Goebel WD, James MJ, Brunden KR, Wilson DA, Landreth GE. ApoE-Directed Therapeutics Rapidly Clear  $\beta$ -Amyloid and Reverse Deficits in AD Mouse Models. *Science.* 2012;335(6075):1503-1506.
24. Coffman VC, Wu P, Parthun MR, Wu JQ. CENP-A exceeds microtubule attachment sites in centromere clusters of both budding and fission yeast. *J Cell Biol.* 2011;195(4):563-72.
25. Liu T, Lin Y, Wen X, Jorissen RN, Gilson MK. BindingDB: A web-accessible database of experimentally determined protein-ligand binding affinities. *Nuc Acids Res.* 2007;35:D198-D201.
26. Chemplus: Modular Extensions for HyperChem Release 6.02, Molecular Modeling for Windows, HyperClub, Inc., Gainesville; 2000.
27. Codding JP. Structure-Based Drug Design: Experimental and Computational Ed. German: Springer; 1998.
28. Almeida JR. Estudos de modelagem molecular e relação estrutura-atividade da acetilcolinesterase e inibidores em Mal de Alzheimer. Dissertação (Mestrado em Ciências), Universidade de São Paulo, Ribeirão Preto; 2011. Portuguese.
29. Sanner MF. Python: A programming language for software integration and development. *J Mol Graph Model.* 1999; 17(1):57-61.
30. Schneidman-Duhovny D, Dror O, Inbar Y, Nussinov R, Wolfson HJ. PharmaGist: A webserver for ligand-based pharmacophore detection. *Nucl Acids Res.* 2008;36:223-228.
31. Dror O, Shulman-Peleg A, Nussinov R, Wolfson HJ. Predicting molecular interactions in silico: I. A guide to pharmacophore identification and its applications to drug design. *Curr Med Chem.* 2004;11(1):71-90.
32. Lee SP, Falangola MF, Nixon RA, Duff K, Helpert JA. Visualization of beta-amyloid plaques in a transgenic mouse model of Alzheimer's disease using MR microscopy without contrast reagents. *Magn Reson Med.* 2004;52(3):538-44.
33. Yamashita F, Hashida M. In silico approaches for predicting ADME properties of drugs. *Drug Metab Pharmacokinet.* 2004;19(5):327-38.
34. Boda K, Seidel T, Gasteiger J. Structure and reaction based evaluation of synthetic accessibility. *J Comput Aided Mol Des.* 2007;21(6):311-325.
35. Filimonov DA, Poroikov VV. Pass: Computerized prediction of biological

- activity spectra for chemical substances. In: *Bioactive Compound Design: Possibilities for Industrial Use*. Oxford: BIOS Scientific Publishers; 1996.
36. Lipinski CA, Lombardo F, Dominy BW, Feeney PJ. Experimental and computational approaches to estimate solubility and permeability in drug discovery and development settings. *Adv Drug Deliv Rev.* 1997;23:3-25.
  37. Cole JC, Murray CW, Nissink JWM, Taylor RD, Taylor R. Comparing Protein–Ligand Docking Programs Is Difficult. *Proteins: Struct, Func Bioinf.* 2005;60:325–332.
  38. Darshit BS, Balaji B, Rani P, Ramanathan M. Identification and in vitro evaluation of new leads as selective and competitive glycogen synthase kinase-3 $\beta$  inhibitors through ligand and structure based drug design. *J Mol Graph Model.* 2014;53:31-47.
  39. Balakrishnan N, Raj JS, Kandakatla N. 2D/3D-QSAR, Docking and optimization of 5-substituted-1h-indazole as inhibitors of GSK-3 $\beta$ . *Int J Pharm Sci.* 2014;6(10):413-420.
  40. Pauling L. *The nature of Chemical Bond: An Introduction to Modern Structural Chemistry*. 4<sup>th</sup> ed. New York: Cornell University Press; 1960.
  41. Ziolkowski M, Grabowski SJ, Leszczynski J. Cooperativity in hydrogen-bonded interactions: Ab Initio and “Atoms in Molecules” Analyses. *J Phys Chem A.* 2006;110(20):6514-6521.
  42. Silva AM. Efeitos de ligações de hidrogênio em propriedades de aglomerados de moléculas interestelares. *Dissertação (Mestrado em Física), Universidade Federal do Amazonas, Amazonas; 2008. Portuguese.*
  43. Bidon-Chanal A, Fuertes A, Alonso D, Pérez DI, Martínez A, Luque FJ, Medina M. Evidence for a new binding mode to GSK-3: Allosteric regulation by the marine compound palinurin. *Eur J Med Chem.* 2013;60:479-489.
  44. Agrawal R, Jain P, Dikshit SN, Bahare RS, Ganguly S. Ligand-based pharmacophore detection, screening of potential pharmacophore and docking studies, to get effective glycogen synthase kinase inhibitors. *Med Chem Res.* 2013;22:5504-5535.
  45. Güner OF. *Pharmacophore perception, development and use in drug design*. Los Angeles: International University Line; 2000.
  46. Taha MO, Bustanji Y, Al-Ghussein MAS, Mohammad M, Zalloum H, Al-Masri IM, Atallah N. Pharmacophore modeling, quantitative structure-activity relationship analysis, and in silico screening reveal potent glycogen synthase kinase-3 $\beta$  inhibitory activities for cimetidine, hydroxychloroquine, and gemifloxacin. *J Med Chem.* 2008;51:2062-2077.
  47. Muster W, Breidenbach A, Fischer H, Kirchner S, Muller L, Pahler A. Computational toxicology in drug development. *Drug Discov Today.* 2008;13:303-310.
  48. Merlot C. Computational toxicology-a tool for early safety evaluation. *Discov Today.* 2009;15(1-2):16-22.
  49. Manallack DT. The pKa distribution of drugs: Application to drug discovery. *Perspect Med Chem.* 2007;1:25-38.
  50. Abraham MH. Human Intestinal Absorption-Neutral Molecules and Ionic Species. *DDDI.* 2014;103:1956-1966.
  51. Zhang P, Hu H, Bia S, Huang Z, Chu Y, Ye D. Design, synthesis and biological evaluation of benzothiazepinones (BTZs) as novel non-ATP competitive inhibitors of glycogen synthase kinase-3 $\beta$  (GSK-3 $\beta$ ). *Eur J Med Chem.* 2013;61:95-103.
  52. Guangli M, Yiyu C. Predicting Caco-2 permeability using support vector machine and chemistry development kit. *J Pharm Pharmaceut Sci.* 2006;9:210-221.
  53. Castillo-Garit JA, Cañizares-Carmenate Y, Marrero-Ponce TF, Abad C. Prediction of ADME properties, Part 1: Classification models to predict Caco-2 cell permeability using atom-based bilinear indices. *Afinidad.* 2014;71(566):129-138.
  54. Irvine JD, Takahashi L, Lockhart K, Cheong J, Tolan JW, Selick HE, Grove JR. MDCK (Madin–Darby Canine Kidney) Cells: A Tool for Membrane Permeability Screening. *J Pharma Sci.* 1999;88(1):28-33.
  55. Volpe DA. Drug-permeability and transporter assays in Caco-2 and MDCK cell lines. *Future Med Chem.* 2011;3:2063-2077.
  56. Nerkar AG, Sahu M. In silico screening, synthesis and in vitro evaluation of some quinazolinone derivatives as dihydrofolate reductase inhibitors for anticancer activity: part-I. *Int J Pharm Sci.* 2014;6:193-199.

57. Xia XR. Quantitative Structure–Permeability Relationships. In: Riviere, J.E. (Ed.), *Comparative Pharmacokinetics: Principles, Techniques, and Applications*. Oxford: John Wiley & Sons, Inc; 2011.
58. Chen L, Han L, Lian G. Recent advances in predicting skin permeability of hydrophilic solutes. *Adv Drug Deliv Rev*. 2013;65:295-305.
59. Alves VM, Muratov E, Fourches D, Strickland J, Kleinstreuer N, Andrade CH, Tropsha A. Predicting chemically induced skin reactions. Part II: QSAR models of skin permeability and the relationships between skin permeability and skin sensitization. *Toxicol Appl Pharmacol*; 2015 (In press).
60. Colmenarejo G. In silico prediction of plasma and tissue protein binding. In: Taylor JB, Triggle DJ. *Comprehensive Medicinal Chemistry II*, v. 5. Oxford: Elsevier; 2007.
61. Jambhekar SS. Physicochemical and biopharmaceutical properties of drug substances and pharmacokinetics. In: Foye WO, Lemke TL, Williams DA editors. *Foye's Principles of Medicinal Chemistry*. New York: Lippincott Williams and Wilkins; 2008.
62. Ghafourian T, Amin Z. QSAR Models for the prediction of plasma protein binding. *Bioimpacts*. 2013;3:21-27.
63. Ma X, Chen C, Yang J. Predictive Model of Blood-Brain Barrier Penetration of Organic Compounds. *Acta Pharmacol. Sin*. 2005; 26:500-512.
64. Goodwin J, Clark, DE. In silico predictions of blood–brain barrier penetration: Considerations to “keep in mind”. *J Pharmacol Exp*. 2005;315(2):477-483.
65. Mensch J, Oyarzabal J, Mackie C, Augustijns P. *In vivo*, *In vitro* and in silico methods for small molecule transfer across the BBB. *J Pharm Sci*. 2009;98:4429-4468.
66. Lanevskij K, Dapkunas J, Juska L, Japertas P, Didziapetris R. QSAR Analysis of Blood–Brain Distribution: The Influence of Plasma and Brain Tissue Binding. *J Pharm Sci*. 2011;100(6):2147-2160.
67. Brito AJ, Raj TLS, Chelliah DA. Prediction of Biological Activity Spectra for Few Anticancer Drugs Derived from Plant Sources. *Ethnobot Leaflets*. 2001;12:801-810.
68. Lagunin A, Stepanchikova A, Filimonov D, Poroikov V. PASS: prediction of activity spectra for biologically active substances. *Bioinformatics*. 2000;16:747-748.

© 2015 Picanço et al.; This is an Open Access article distributed under the terms of the Creative Commons Attribution License (<http://creativecommons.org/licenses/by/4.0>), which permits unrestricted use, distribution, and reproduction in any medium, provided the original work is properly cited.

*Peer-review history:*

*The peer review history for this paper can be accessed here:*  
<http://www.sciencedomain.org/review-history.php?iid=1178&id=14&aid=9586>